*Revue des Energies Renouvelables Vol. 15 N°3 (2012) 383 - 397*

# Performance evaluation of a GaSb thermophotovoltaic converter

F. Bouzid * and L. Dehimi

Laboratory of Metallic and Semiconducting Materials
Mohamed Khider University, B.P. 145, Biskra, Algeria

(reçu le 15 Novembre 2011 – accepté le 30 Septembre 2012)

**Abstract** – *In recent years, Gallium Antimonide (GaSb), which has smallest bandgap among III-V semiconductors family, became the subject of extensive investigations in the field of thermophotovoltaic (TPV) converters, because of the recent improvements in optoelectronic technology. This paper describes an analytical process used to evaluate the performance of a GaSb TPV converter under different levels of illumination, taking account of the photons with energy below the cells bandgap by considering the cell's reflectance to this fraction of incident radiation. The results show that a radiator temperature near 2200 K is most advantageous and a reflectance of 0.98 is necessary for below-bandgap irradiations to obtain conversion efficiency greater than 28%, at 300 K cell temperature. This efficiency will decrease as the cell temperature increase. The obtained results are found to be in good agreement with the available data.*

**Résumé** – *Ces dernières années, l'antimoniure de gallium (GaSb), qui a le plus petit gap énergétique dans la famille des semi-conducteurs III-V, est devenu le sujet d'investigations étendues dans le domaine des convertisseurs thermophotovoltaïques (TPV), en raison des améliorations récentes en technologie optoélectronique. Cet article décrit un processus analytique employé pour évaluer la performance d'un convertisseur thermophotovoltaïque (TPV) à base de GaSb sous différents niveaux d'illumination, en tenant compte des photons avec énergie au-dessous du gap énergétique des cellules en considérant la réflectivité des cellules à cette fraction du rayonnement incident. Les résultats montrent qu'une température du radiateur près de 2200 K est très avantageuse et une réflectivité de 0.98 est nécessaire pour les radiations au-dessous du gap énergétique pour obtenir un rendement de conversion supérieur à 28%, à la température 300 K de la cellule. Ce rendement diminuera avec l'augmentation de la température de la cellule. Les résultats obtenus s'avèrent en bon accord avec les données disponibles.*

**Keywords**: Thermophotovoltaic - GaSb - Reflectance - Emissivity - Temperature.

## 1. INTRODUCTION

The investigations in the field of TPV converters started in the early 1960s, but the real advantage of the TPV approach has been demonstrated only in the past two decades [1].

Thermophotovoltaic converters are devices in which a photovoltaic (PV) device converts the radiation emitted by heated body into electric power [2]. The radiator, generally made by refractory materials such as tungsten [3] or ceramic oxides [4], may be heated by the ignition of a fuel, radio isotopic power sources or by using highly concentrated sunlight as described in figure 1.

* faycal.bouzid@ymail.com

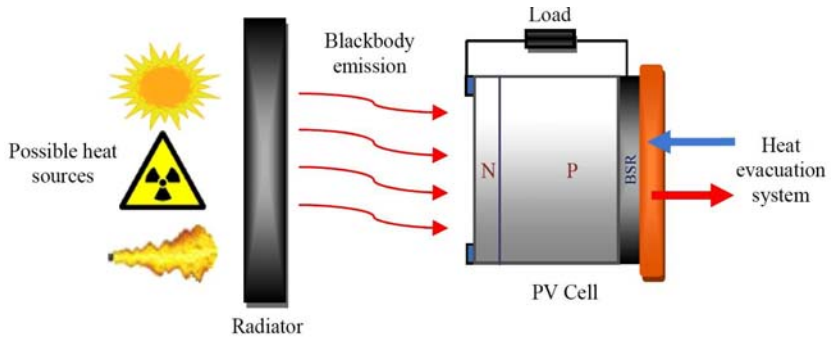


Fig. 1: Principle of thermophotovoltaic conversion

In order to make the process efficient, the energy of the photons reaching the PV cell must be superior to the bandgap energy of the cell. For this reason, GaSb and its related ternary and quaternary alloys have been considered as promising materials for TPV applications because of their low bandgap energies. These cells are able to convert a larger part of the infrared spectrum, and therefore have the potential to give high efficiency and power output at moderate radiator temperature.

To increase the efficiency which is determined by energy absorbed relative to total incoming radiation, the remainder of the spectrum must be reflected back to the radiator. Thereby a back surface reflector (BSR) is often employed in the design of conventional TPV cells. This creates the concept of 'photon recycling' whereby photons with energies less than optimum for conversion are sent back to the radiator for recycling until they come back at the proper energy [5].

The current TPV cell technology is approaching 30% cell efficiency at 300 K due steady improvement in MOCVD manufacturing process. Through the use of dual junction cells to convert below bandgap photons, further improvements in the cell efficiency are expected to take place over the next few years with expectations of approaching 40% [6].

In this work, the theoretical efficiency of GaSb TPV converter is computed using a comprehensive model in which the cells are exposed to radiation from a blackbody radiator in the 1300 K to 2200 K temperature range. The influence of the base region doping profile, the cell thickness, the reflectance, the radiator emissivity and the cell temperature on the conversion efficiency have been investigated.

These theoretical calculations help us to better understand the electro-optical behavior of GaSb TPV cells and can be utilized for performance enhancement through optimization of the device structure.

## 2. MODEL DESCRIPTION

Figure 2 show a simplified structure of a GaSb TPV cell, where xj is the junction depth, w is the depletion region width, h is the P-type quasi neutral region and d is the cell thickness.

In our calculations, the effect of the back surface field (BSF) is not taken into account for the sake of simplicity, no structural losses and contact shadowing for the cells and the values of the physical and geometrical parameters were chosen from various published papers.

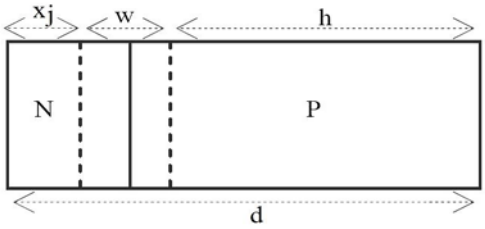


Fig. 2: Simplified configuration of a GaSb TPV cell

**2.1 Analytical model**

The determination of the TPV cell efficiency implies knowledge of its current voltage characteristic under illumination which can be written as [7]:

$$I_{Total} = I_{Ph} - I_D \tag{1}$$

where $I_D$ is the dark current (in the absence of irradiation), and $I_{Ph}$ is the current excited by the incident radiations, i. e., the photocurrent for the so-called ideal model.

The dark current is described by the Shockley diode equation:

$$I_D = I_0 \times \left[ \exp\left( \frac{q \times V}{k \times T} \right) - 1 \right] \tag{2}$$

where $q$ is the elementary charge, $k$ is the Boltzmann constant, $T$ is the temperature and $I_0$ is the reverse saturation current, given by equation (3) [7], using the cell design shown in figure 2:

$$I_0 = \frac{q S D_e n_i^2}{I_e N_a} \times \frac{\frac{S_e I_e}{D_e}\cosh\left(\frac{h}{I_e}\right) + \sinh\left(\frac{h}{I_e}\right)}{\frac{S_e I_e}{D_e}\sinh\left(\frac{h}{I_e}\right) + \cosh\left(\frac{h}{I_e}\right)} + \frac{q S D_h n_i^2}{I_h N_d} \times \frac{\frac{S_h I_h}{D_h}\cosh\left(\frac{x_j}{I_h}\right) + \sinh\left(\frac{x_j}{I_h}\right)}{\frac{S_h I_h}{D_h}\sinh\left(\frac{x_j}{I_h}\right) + \cosh\left(\frac{x_j}{I_h}\right)} \tag{3}$$

where $n_i$ is the intrinsic carrier concentration calculated from the relation:

$$n_i^2 = N_c N_v \times \exp\left( -\frac{E_g}{k T} \right) \tag{4}$$

where $N_c$ and $N_v$ are the effective densities of states in the conduction and valence bands respectively, $E_g$ is the bandgap energy, $N_a$ and $N_d$ are the acceptor and donor concentrations, $S_h$ and $S_e$ are the recombination velocities in the $N$ and $P$-type regions, $S$ is the cell surface, $D_e$ and $D_h$ are the diffusion constants of electrons and holes respectively, calculated from Einstein relationship:

$$D_{e/h} = \frac{kT}{q} \times \mu_{e/h} \tag{5}$$

where $\mu_e$ and $\mu_h$ are mobilities of the electrons and holes respectively, $l_e$ and $l_h$ are the minority carrier diffusion lengths of electrons and holes respectively.

The photocurrent $I_{Ph}$ is given by the sum of the photocurrents generated in the emitter, the base and the depleted region of the cell.

$$I_{Ph} = \int_0^{\lambda_{max}} q \times S \times F(\lambda) \times SR(\lambda) \times d\lambda \tag{6}$$

where $\lambda$ is the wavelength of the incident photon, $\lambda_{max}$ is the cutoff wavelength corresponding to the bandgap energy, and $SR(\lambda)$ is the internal spectral response of the TPV cell given by the sum of the contribution from the emitter, the base and the depleted region as described in equation (7):

$$SR(\lambda) = SR_E(\lambda) + SR_B(\lambda) + SR_{DR}(\lambda) \tag{7}$$

$F(\lambda)$ is the spectral photons flux of the incident radiation that was absorbed by the TPV cell. Its expression for $\lambda < \lambda_{max}$ could be written as [8, 9]:

$$F(\lambda) = \chi \times \frac{2\pi \times c}{\lambda^4 \times \left( e^{\frac{hc}{\lambda k T_{Rad}}} - 1 \right)} \tag{8}$$

where $T_{Rad}$ is the TPV radiator temperature, $h$ is the plank constant, $c$ is the speed of light and $\chi$ is the effective cavity emissivity that characterizes the performance of the spectral control in TPV system. The value of $\chi$ is taken as 0.78 based on the best reported spectral control system performance.

### 2.2 Photovoltaic parameters

The open circuit voltage is expressed as [7]:

$$V_{oc} = \frac{n k T_{cel}}{q} \times \ln\left( \frac{I_{sc}}{I_0} + 1 \right) \tag{9}$$

where $n$ is the factor of ideality assumed to be 1 for GaSb TPV cells based on [10], $I_{sc}$ is the short circuit current, and $T_{Cel}$ is the cell temperature.

The power delivered by the cell is given by the product of the cell voltage and current, and was maximized by satisfying the condition:

$$\frac{d(I_{Total} \times V)}{dI} = 0 \tag{10}$$

The overall conversion efficiency of a TPV system can be expressed as [11]:

$$\eta = \frac{\eta_{Cel}}{1 - f_t \times \rho} c \tag{11}$$

where $f_t$ is the fraction of the spectrum below the cell's bandgap, $\rho$ is the cell reflectance to the radiation with energy below the cell's bandgap, and $\eta_{Cel}$ is the cell efficiency expressed as [7]:

$$\eta_{Cel} = \frac{I_m \times V_m}{P_{Inc}} \tag{12}$$

where $P_{Inc}$ is the total incident radiation power integrated over all frequencies, $I_m$ and $V_m$ are coordinates of the maximum power point.

The fill factor is defined by:

$$FF = \frac{I_m \times V_m}{I_{sc} \times V_{oc}} \tag{13}$$

**2.3 GaSb parameter equations**

Ferguson *et al.* [10] suggested a semi empirical equation for the temperature dependence of the bandgap energy of the form:

$$E_g = 0.813 - \frac{(6 \times 10^{-4}) \times T^2}{(T + 265)} \tag{14}$$

This equation was based on the observation that the energy gap should be proportional to $T$ at high temperatures and proportional to $T^2$ at low temperatures.

Mobilities of the electrons and holes are calculated as a function of doping and temperatures using the Caughey – Thomas empirical model [12-14] given as:

$$\mu_{e/h}(N_{a/d}, T_{Cel}) = \mu_{min,e/h} + \frac{\mu_{max,e/h} \times (300/T_{Cel})^{\theta_{1},e/h} - \mu_{min,e/h}}{1 + \left[ N_{a/d}/N_{ref,e/h} \times (T_{Cel}/300)^{\theta_{2},e/h} \right]^{\alpha_{e/h}}} \tag{15}$$

where $\mu_{min,e/h}$ and $\mu_{max,e/h}$ represents the value that mobility reaches for very low and high doping level, $N_{ref,e/h}$ is the doping concentration at which the mobility is decreased to half the value is reaches at low doping at room temperature. $\theta_{1,e/h}$, $\theta_{2,e/h}$ and $\alpha e/h$ are respectively the suggested fitting parameters [12].

All the value of parameters used for the simulation of the carrier mobilities has been summarized in **Table 1**.

The absorption coefficient of GaSb was calculated using the direct bandgap semi-conductor expression given as [15]:

$$\alpha(E) = K_{abs} \times \sqrt{(E - E_g)} \quad (16)$$

**Table 1**: Parameters used in the simulation of GaSb carrier mobilities

| | $\mu_{min,e}$ $cm^2/vs$ | $\mu_{max,e}$ $cm^2/vs$ | $\mu_{min,h}$ $cm^2/vs$ | $\mu_{max,h}$ $cm^2/vs$ | $\theta_{1,e}$ | $\theta_{1,h}$ |
|---|---|---|---|---|---|---|
| **GaSb** | 1050 | 5650 | 190 | 875 | 2 | 1.7 |
| | $\theta_{2,e}$ | $\theta_{2,h}$ | $\alpha_e$ | $\alpha_h$ | $N_{ref,e}$ $cm^{-3}$ | $N_{ref,h}$ $cm^{-3}$ |
| **GaSb** | 2.8 | 2.7 | 1.05 | 0.65 | $2.8e^{17}$ | $9e^{17}$ |

$$K_{abs} = \frac{q^2 \times \chi_{vc}^2 \times (2m_r)^{3/2}}{\lambda_{max} \times \varepsilon_0 \times \hbar^3 \times n_{op}} \quad (17)$$

$$\chi_{vc} = \frac{\hbar}{E_g} \times \sqrt{\frac{E_p}{3m_0}} \quad (18)$$

where $E$ is the incoming photon energy, $E_p$ is the Kane's energy, $m_0$ is the electron rest mass, $n_{op}$ is the optical refraction index and $m_r$ is the reduced effective mass.

The specific parameters $\chi_{vc}$, $m_r$, $\lambda_{max}$ and $n_{op}$ used in the simulation are given in **Table 2**.

**Table 2**: Specific parameters used to calculate the absorption coefficient of GaSb

| $\chi_{vc}$ **(A°)** | $m_r$ | $\lambda_{max}$ **(m)** | $n_{op}$ **[16]** | $\xi_0$ **(F/m)** |
|---|---|---|---|---|
| **2.63** | 0.043 | $1.72e^{-6}$ | 3.8 | $8.85e^{-12}$ |

The relative dielectric constant of GaSb is taken to be 15.7 [15].

The effective masses for electrons and holes are given by the expressions:

$$m_e^* = 0.047 \times m_0 \quad [15] \quad (19)$$

$$m_h^* = 0.5 \times m_0 \quad [17] \quad (20)$$

The effective densities of states $N_c$ and $N_v$ are given in [18] as:

$$N_c = 4 \times 10^{13} \times T^{1.5} \quad (21)$$

$$N_v = 3.5 \times 10^{15} \times T^{1.5} \quad (22)$$

**2.4 Incident light spectrum**

Figure 3 gives a general idea of how much light is accessible to a PV cell made of GaSb. The colored portions in the figure indicate the fraction of the photon spectrum that is above the bandgap energy.

**Table 3** below indicates the fraction of incident light with energies below the cell's bandgap calculated by integrating the spectral irradiance under the blackbody curve for $\lambda > \lambda_{max}$ , and the total incident radiation power $P_{Inc}$ .

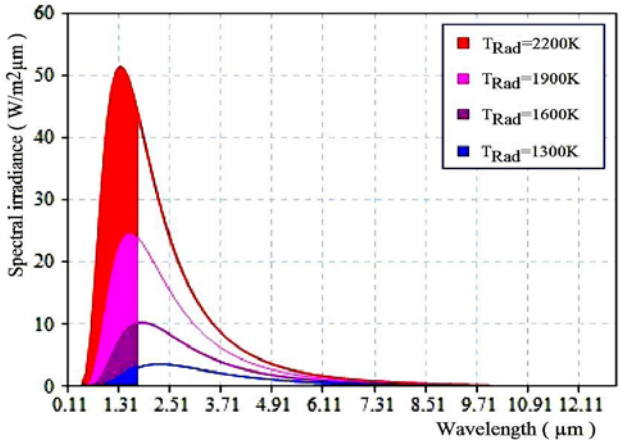


Fig. 3: Blackbody spectral irradiance for $\chi = 0.78$

**Table 3**: Percentage of incident radiations with energies below the GaSb bandgap for $\chi = 0.78$, and the total incident radiation power $P_{Inc}$

| $T_{Rad}$ **(K)** | 1300 | 1600 | 1900 | 2200 |
|---|---|---|---|---|
| $f_t$ **(%)** | 89.28 | 78.39 | 66.82 | 56.11 |
| $P_{Inc}$ **(W/m²)** | 12.5 | 28.9 | 57.5 | 103.4 |

## 3. RESULTS AND DISCUSSION

### 3.1 Effect of the base region profile and cell thickness

The level of doping plays a crucial role in the performance of TPV devices. To reveal the potential effect brought by the base region doping profile, we have simulated and plotted the conversion efficiency versus different doping levels in figure 4.

**Table 4**: Cell parameters used in simulations at $T_{Cel} = 300$ K

| $T_{Rad}$ (K) | $\chi$ | $\rho$ | $E_g$ eV | $S_e$ cm/s | $S_h$ cm/s | $x_j$ µm |
|---|---|---|---|---|---|---|
| **2200** | 0.78 | 0.98 | 0.72 | 4000 | 200 | 0.5 |
| $N_d$ **cm⁻³** | $N_{TD}$ cm⁻³ | $N_{TA}$ cm⁻³ | $V_{te}$ cm/s [18] | $V_{th}$ cm/s [18] | $\sigma_e$ cm² [19] | $\sigma_h$ cm² [19] |

| | | | | | | |
|---|---|---|---|---|---|---|
| **$2e^{18}$** | $2.15e^{16}$ | $5.3e^{12}$ | $5.8e^{7}$ | $2.e^{7}$ | $8e^{-19}$ | $9e^{-15}$ |

The analysis starts by assuming the values assigned for the cell parameters, presented in **Table 4**, where $N_{TD}$ and $N_{TA}$ are the concentrations of donor and acceptor traps, $V_{te}$ and $V_{th}$ are the thermal velocities for electrons and holes, $\sigma_e$ and $\sigma_h$ are the capture cross sections for electrons and holes respectively.

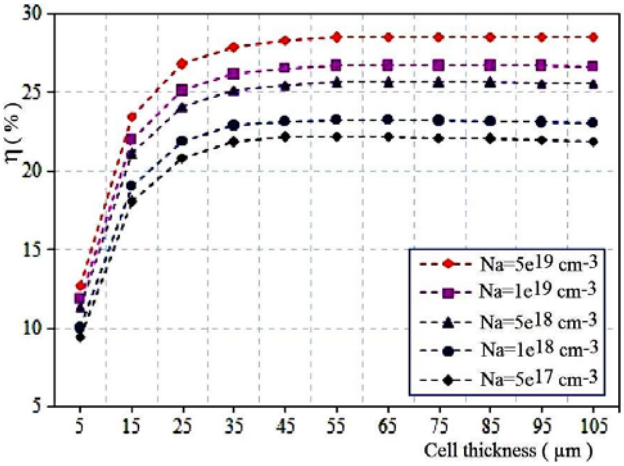


Fig. 4: Effect of the base region profile
and cell thickness on the conversion efficiency

It can be seen from figure 4 above that the maximum value of the base region doping concentration is about $5e^{19}$ $cm^{-3}$. At the same time, it is clear that the efficiency increases significantly with increasing the cell thickness. Where, in case of $Na = 5e^{19}$ $cm^{-3}$, the efficiency curve shows an improvement from 12.72 % to 28.56 % for 5 µm and 75 µm cell's thickness respectively for the reason that, in case of too thin thickness, most of the incident photons are not absorbed resulting in a lower efficiency.

However, when the cell thickness exceeds 75 µm, we note a weak reduction in the conversion efficiency due to the recombination phenomenon, since the free carriers generated deeper in the bulk have to travel longer before being collected. So a cell thickness of about 75 µm is needed to lose not too much of the efficiency.

### 3.2 Effect of the front recombination velocity

In this work, the back surface recombination velocity was fixed at 4000 cm/s, and the influence of the front recombination velocity on the conversion efficiency has been simulated, where values of 200, 500, 1000 and 2000 cm/s was used for different cell thicknesses with $T_{Rad} = 2200$ K, $T_{cell} = 300$ K, $N_a = 5e^{19}$ $cm^{-3}$, $\chi = 0.78$ and $\rho = 0.98$.

From figure 5 below, it is apparent that the efficiency drops notably with increasing the front recombination velocity, particularly for high cell thicknesses, since most of the photo-generated carriers cannot be collected by the electrodes what implies a low electric current. The maximum conversion efficiency obtained for 75 µm cell thickness can attain 28.56 % for a front recombination velocity equals to 200 cm/s. Therefore, to

reduce the power loss, the front surface recombination velocity should not exceed 200 cm/s.

### 3.3 Effect of the cell reflectance

We simulated the effect that cell reflectance would have on the conversion efficiency for different radiator's temperature, and the results were shown in figure 6.

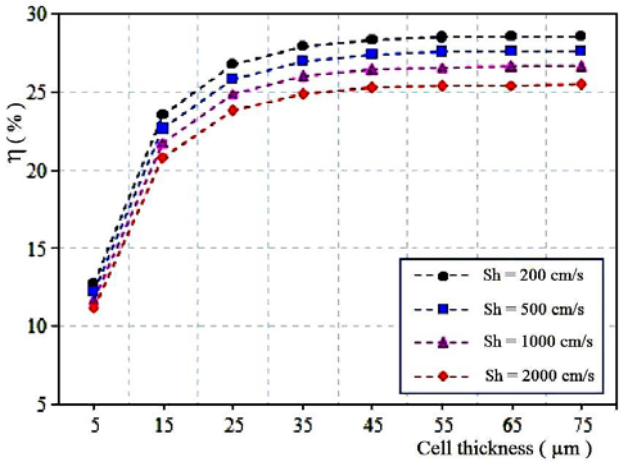


Fig. 5: Effect of the front surface recombination velocity and cell thickness on the conversion efficiency

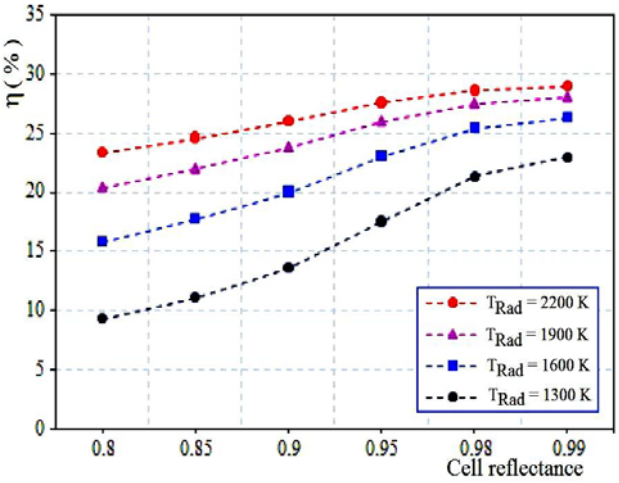


Fig. 6: Effect of the cell reflectance on the conversion efficiency for $T_{Cel}$ = 300 K, $N_a$ = 5e$^{19}$ cm$^{-3}$ and $\chi$ = 0.78

As it is expected, the conversion efficiency becomes more important as the reflectance to radiations below the cell's bandgap increases, particularly for low radiator temperatures, for the reason that a larger fraction of the emitted spectrum is below the

cell's bandgap. Thus, a cell reflectance value of 0.98 is required to attain high conversion efficiencies, since values greater than 0.98 are not realistic.

### 3.4 Effect of the radiator effective cavity emissivity

It is interesting to evaluate the average emissivity-dependant effect on the practical device performance.

In figure 7, we have simulated the current-voltage characteristics as a function of $\chi$, while **Table 5** gives the computations of the open circuit voltage, short circuit current, fill factor and the conversion efficiency for all cases of the radiator effective emissivity with $T_{Rad} = 2200$ K, $T_{Cel} = 300$ K, $N_a = 5e^{19}$ $cm^{-3}$and $\rho = 0.98$.

**Table 5**: Effect of the radiator emissivity on the photovoltaic parameters

| $\chi$ | 0.5 | 0.6 | 0.7 | 0.8 | 0.9 |
|---|---|---|---|---|---|
| $V_{oc}$ (V) | 0.432 | 0.438 | 0.443 | 0.446 | 0.499 |
| $I_{sc}$ (A) | 2.43 | 2.92 | 3.41 | 3.89 | 4.38 |
| FF (%) | 78.20 | 78.42 | 78.55 | 78.58 | 78.77 |
| $\eta$ (%) | 27.69 | 28.05 | 28.37 | 28.60 | 28.85 |

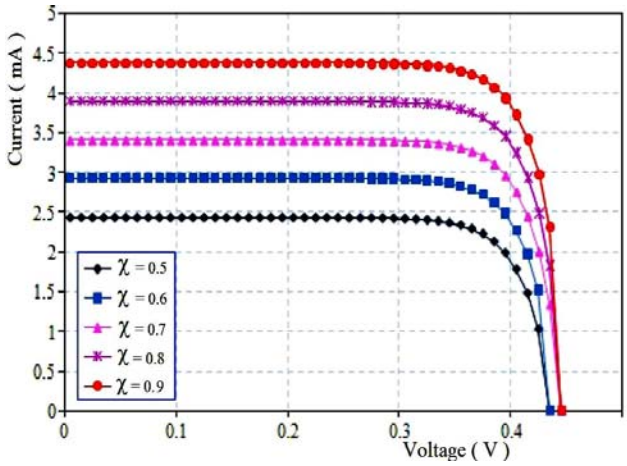


Fig. 7: Simulated current-voltage characteristics for different values of the effective emissivity

It is seen, from the table and the figure above, that the efficiency improves from 27.69 % for $\chi$ = 0.5 to 28.85 % for $\chi$ = 0.9. Both open circuit voltage and the fill factor show little increment with the evolution of $\chi$, whereas, the remaining parameters displays important improvements.

These results are very similar to those obtained by Khvostikov *et al.* [20]. They measured the conversion efficiency of GaSb cells fabricated by the optimized Zn diffusion method and they obtained efficiencies of 27-28 % at black body temperature > 2000 K. Therefore, it is very important to enhance the radiator's emissivity by developing new materials and designs.

### 3.5 Effect of the radiator temperature

We simulated the current-voltage characteristic under four types of blackbody illumination spectrums with $T_{Cel}$ = 300 K, $N_a$ =5e$^{19}$ cm$^{-3}$, $\chi$ = 0.78, $\rho$ = 0.98, and the results were shown in figure 8. **Table 6** shows that the efficiency improves from 21.27% to 28.56 % for 1300 K and 2200 K radiator's temperature respectively.

This improvement can be explained by taking into account that the increase in the radiator's temperature involves a significant increase in photocurrent for the reason that, as we saw in equation (6), the photocurrent is practically proportional to luminous flow, and owing to the fact that the open circuit voltage is also related to the short circuit current, it will undergo an increase and the conversion efficiency is always better in case of 2200 K radiator's temperature.

**Table 6**: Effect of the radiator temperature on the photovoltaic parameters

| $T_{Rad}$ (K) | 1300 | 1600 | 1900 | 2200 |
|---|---|---|---|---|
| $V_{oc}$ (V) | 0.36 | 0.39 | 0.42 | 0.44 |
| $I_{sc}$ (A) | 0.12 | 0.56 | 1.65 | 3.80 |
| FF (%) | 75.14 | 76.84 | 77.82 | 78.56 |
| $\eta$ (%) | 21.27 | 25.38 | 27.49 | 28.56 |

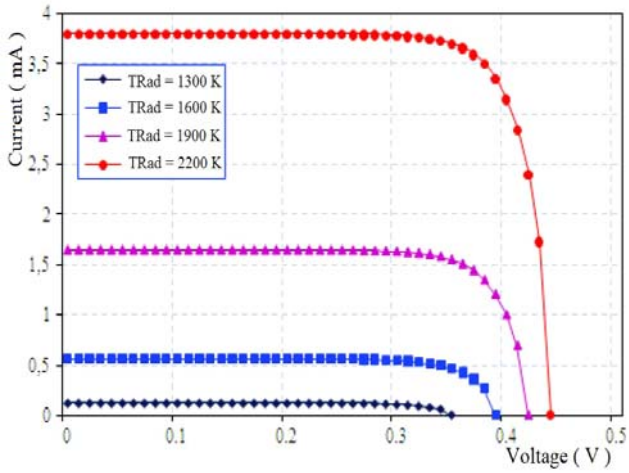


Fig. 8: Simulated current-voltage characteristics under four types of blackbody illumination spectrums

### 3.6 Effect of the cell temperature

As it is not realistic to operate a TPV cell at 300 K, we have simulated the effect of elevated operating temperatures on the performance of the converter for Na = 5e$^{19}$ cm$^{-3}$, $\chi$ = 0.78 and $\rho$ = 0.98, under four types of blackbody illumination spectrums.

According to the results represented in **Table 7** and the figures 9, 10 and 11 below, it is seen that the increase of the cell's temperature causes a reduction in the bandgap width, therefore, the reverse saturation current will increase, causing a reduction in the open circuit voltage, and the mechanism of carrier's production becomes increasingly

significant what implies a weak increase in the short circuit current, in case of low radiator's temperature, and more significant increase in the short circuit current for elevated radiator's temperature.

It may be seen also that the fill factor undergoes a reduction with the increase of the cell's temperature following the increase in the dark saturation current, and owing to the fact that the reduction in the open circuit voltage is more significant with respect to the increase of the short circuit current, the conversion efficiency will also decrease as shown in figure 12.

**Table 7**: Effect of the cell temperature on the photovoltaic parameters

| $T_{Cel}$ | | | | | | | | | | | | |
|---|---|---|---|---|---|---|---|---|---|---|---|---|
| $T_{Rad}$ | 1300 | 1600 | 1900 | 2200 | 1300 | 1600 | 1900 | 2200 | 1300 | 1600 | 1900 | 2200 |
| $E_g$ | 0.72 | 0.72 | 0.72 | 0.72 | 0.70 | 0.70 | 0.70 | 0.70 | 0.68 | 0.68 | 0.68 | 0.68 |
| $I_0$ | $1.26e^{-10}$ | $1.26e^{-10}$ | $1.26e^{-10}$ | $1.26e^{-10}$ | $9.38e^{-9}$ | $9.38e^{-9}$ | $9.38e^{-9}$ | $9.38e^{-9}$ | $2.99e^{-7}$ | $2.99e^{-7}$ | $2.99e^{-7}$ | $2.99e^{-7}$ |
| $V_{oc}$ | 0.36 | 0.39 | 0.42 | 0.44 | 0.28 | 0.32 | 0.36 | 0.38 | 0.20 | 0.25 | 0.29 | 0.31 |
| $I_{sc}$ | 0.12 | 0.56 | 1.65 | 3.80 | 0.14 | 0.62 | 1.80 | 4.07 | 0.16 | 0.68 | 1.93 | 4.32 |
| FF | 75.14 | 76.84 | 77.82 | 78.56 | 68.61 | 71.32 | 72.94 | 74.12 | 59.68 | 64.15 | 66.77 | 68.44 |
| η | 21.27 | 25.38 | 27.49 | 28.56 | 17.53 | 21.46 | 23.56 | 24.67 | 12.41 | 16.37 | 18.65 | 19.92 |

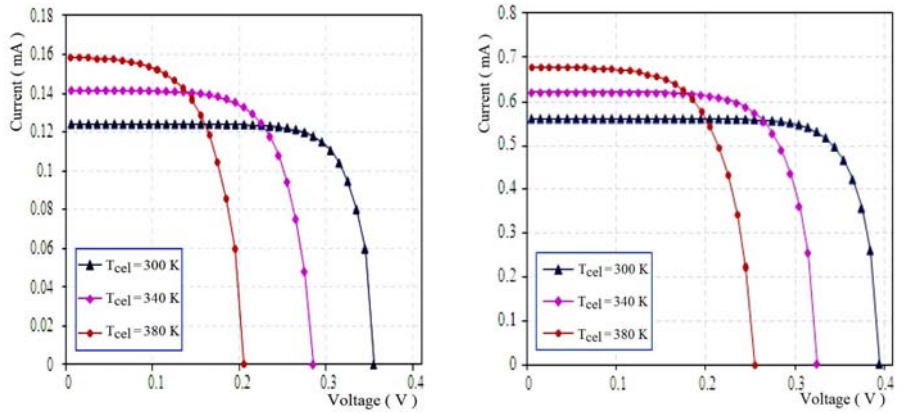


-a- for $T_{Rad}$ = 1300 K -b- for $T_{Rad}$ = 1600 K

Fig. 9: Simulated current-voltage characteristics for different cell temperatures

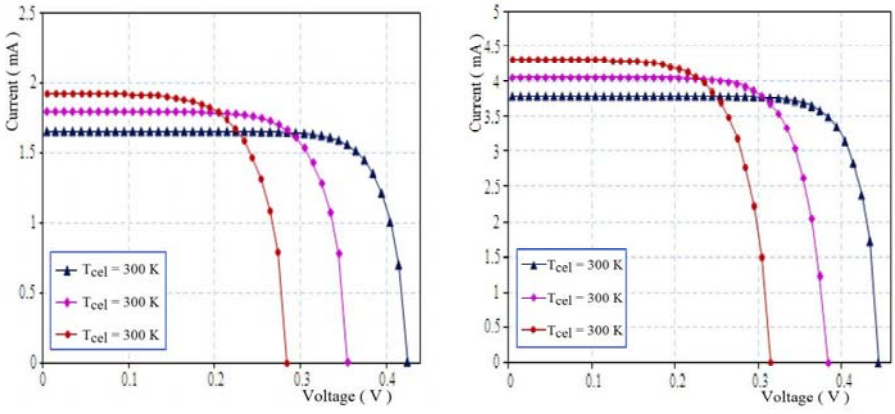


-a- for $T_{Rad}$ = 1900 K -b- for $T_{Rad}$ = 2200 K

Fig. 10: Simulated current-voltage characteristics for different cell temperatures

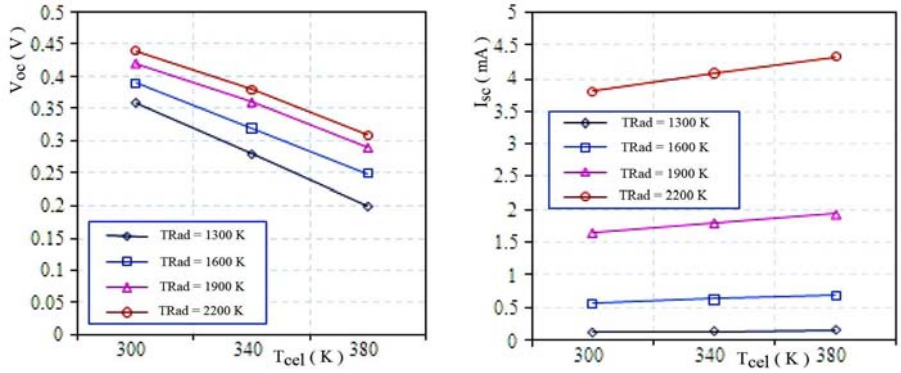


Fig. 11: Variations of the open circuit voltage
and the short circuit current with the cell temperature

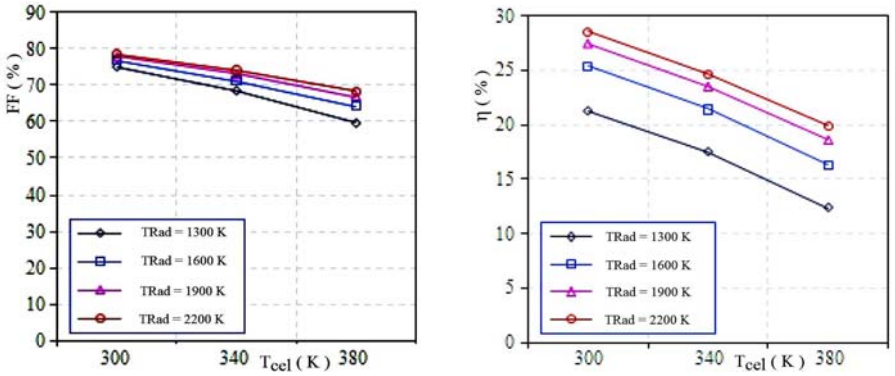


Fig. 12: Variations of the fill factor and

the conversion efficiency with the cell temperature

## 4. CONCLUSION

In this study, we have improved a comprehensive model to predict the performance of a GaSb TPV converter using a simulation program designed for this reason. Our results indicate that in order to achieve higher conversion efficiency, it is important to keep the base region doping as high as possible. Moreover, a cell thickness of about 75 μm with low front recombination velocity and a cell reflectance value of 0.98, for the radiations with energy below the cell's bandgap, are privileged to not contribute significantly in recombination. These results indicate the importance of good contact quality and the BSR in the practical device applications.

It was found also that the conversion efficiency depends not only on the quality of the PV cell itself, but also on other external conditions as the specter quality, which depends strongly of the radiator emissivity and temperature. Our study proves that the spectrums of radiators operating at temperatures greater than 2000 K, for an emissivity value of 0.78, contain significant proportion of incident radiations with energies sufficient to generate charge carriers in the PV cell and efficiencies exceeding 28 % have been achieved by considering the cell's reflectance to the radiations with energy below the cell's bandgap. The obtained results are found to be in good agreement with the available data.

In addition, we have analyzed the effect of elevated cell operating temperature on the conversion efficiency and we found that the increase of the cell temperature results a degradation of their performances.

## REFERENCES

[1] D.L. Chubb, '*Fundamentals of Thermophotovoltaic Energy Conversion*', First Edition, Elsevier Science, 530 p., 2007.

[2] A. Luque and S. Hegedus, '*Handbook of Photovoltaic Science and Engineering*', John Wiley & Sons, 1138 p., 2003.

[3] V.M. Andreev, A.S. Vlasov, V.P. Khvostikov, O.A. Khvostikova, P.Y. Gazaryan, S.V. Sorokina and N.A. Sadchikov, '*Solar Thermophotovoltaic Convertors Based on Tungsten Emitters*', Journal of Solar Energy Engineering, Transactions of the ASME, Vol. 129, N°3, pp. 298-303, 2007.

[4] A. Licciulli, D. Diso, G. Torsello, S. Tundo, A. Maffezzoli, M. Rella and M. Mazzer, '*The Challenge of High-Performance Selective Emitters for Thermophotovoltaic Applications*', Semiconductor Science and Technology, Vol. 18, N°5, pp. 174-183, 2003.

[5] W.M. Yang, S.K. Chou, C. Shu, Z.W. Li and H. Xue, '*Research on Micro-Thermophotovoltaic Power Generators*', Solar Energy Materials and Solar Cells, Vol. 80, N°1, pp. 95-104, 2003.

[6] V.L. Teofilo, P. Choong, J. Chang, Y.L. Tseng and S. Ermer, '*Thermophotovoltaic Energy Conversion for Space*', Journal of Physical Chemistry C, Vol. 112, N°3, pp. 7841-7845, 2008.

[7] S.M. Sze and K.K. Ng, '*Physics of Semiconductor Devices*', Third Edition, John Wiley & Sons, Interscience, 815 p., 2006.

[8] Y. Wang, N.F.Chen, X.W. Zhang, T.M. Huang, Z.G. Yin, Y.S. Wang and H. Zhang, *'Evaluation of Thermal Radiation Dependent Performance of GaSb Thermophotovoltaic Cell*

*Based on An Analytical Absorption Coefficient Model'*, Solar Energy Materials and Solar Cells, Vol. 94, N°10, pp. 1704-1710, 2010.

[9] X. Peng, X. Guo, B. Zhang, X. Li, X. Zhao, X. Dong, W. Zheng and G. Du, '*Numerical Analysis of the Short-Circuit Current Density in GaInAsSb Thermophotovoltaic Diodes*', Infrared Physics and Technology, Vol. 52, N°4, pp. 152 - 157, 2009.

[10] L.G. Ferguson and L.M. Fraas, '*Theoretical Study of GaSb PV Cell Efficiency as a Function of Temperature*', Solar Energy Materials & Solar Cells, Vol. 39, N°1, pp. 11-18, 1995.

[11] M.W. Edenburn, '*Analytical Evaluation of a Solar Thermophotovoltaic (TPV) Converter*', Solar Energy, Vol. 24, N°4, pp. 367- 371, 1979.

[12] D. Martin and C. Algora, '*Temperature-Dependent GaSb Material Parameters for Reliable Thermo-Photovoltaic Cell Modeling*', Semiconductor Science and Technology, Vol. 19, N°8, pp. 1040-1052, 2004.

[13] O.V. Sulima and A.W. Bett, '*Fabrication and Simulation of GaSb Thermophotovoltaic Cells*', Solar Energy Materials and Solar Cells, Vol. 66, N°1-4, pp. 533 - 540, 2001.

[14] D.M. Caughey and R.E. Thomas, '*Carrier Mobility in Silicon Empirically Related to Doping and Field*', Proceedings, IEEE, Vol. 55, pp. 2192 - 2193, 1967.

[15] E. Rosencher and B. Vinter, '*Optoélectronique*', Thomson-CSF, Masson, 1998.

[16] A. Chandola, R. Pino and P.S. Dutta, '*Below Bandgap Optical Absorption in Tellurium-Doped GaSb*', Semiconductor Science and Technology, Vol. 20, N°8, pp. 886 - 893, 2005.

[17] L.L. Li, W. Xu, Z. Zeng, A.R. Wright, C. Zhang, J. Zhang, Y.L. Shi and T.C. Lu, '*Mid-Infrared Absorption by Short-Period InAs/GaSb type II superlattices'*, Microelectronics Journal, Vol. 40, N°4-5, pp. 815 - 817, 2009.

[18] Ioffe Physico-Technical Institute: http://www.ioffe.rssi.ru/SVA/NSM/Semicond/GaSb/bandstr.html

[19] A. Ali, H.S. Madan, A.P. Kirk, D.A. Zhao, D.A. Mourey, M.K. Hudait, R.M. Wallace, T.N. Jackson, B.R. Bennett, J.B. Boos and S. Datta, '*Fermi Level Unpinning of GaSb (100) Using Plasma Enhanced Atomic Layer Deposition of $Al_2O_3$*', Applied Physics Letters, Vol. 97, Issue 14, pp. 143502-1 - 143502-3, 2010.

[20] V.P. Khvostikov, V.D. Rumyantsev, O.A. Khvostikova, M.Z. Shvarts, P.Y. Gazaryan, S.V. Sorokina, N.A. Kaluzhniy and V.M. Andreev, '*Thermophotovoltaic Cells Based on Low-Band gap Compounds'*, 6th Conference on Thermophotovoltaic Generation of Electricity, Freiburg, June 2004.